Parietal regions processing visual 3D shape extracted from disparity

Jean-Baptiste Durand [a,1], Ronald Peeters [b], J. Farley Norman [c], James T. Todd [d], Guy A. Orban [a,*]

[a] Laboratorium voor Neuro- en Psychofysiologie, K.U. Leuven Medical School, Herestraat 49, 3000, Leuven, Belgium
[b] Radiology Department, U.Z. Gasthuisberg, Herestraat, 3000 Leuven, Belgium
[c] Department of Psychology, Western Kentucky University, College Heights Boulevard, Bowling Green, KY 42101, USA
[d] Department of Psychology, Ohio State University, Townshend Hall, Columbus, OH 43210, USA

ARTICLE INFO

ABSTRACT

Three-dimensional (3D) shape is important for the visual control of grasping and manipulation. We used fMRI to study the processing of 3D shape extracted from disparity in human parietal cortex. Subjects stereoscopically viewed random-line stimuli portraying a 3D structure, a 2D structure in multiple depth planes or a 2D structure in the fixation plane. Subtracting the second from the first condition yields depth-structure sensitive regions and subtracting the third from the second position-in-depth sensitive regions. Two anterior intraparietal sulcus (IPS) regions, the dorsal IPS medial (DIPSM) and the dorsal IPS anterior (DIPSA) regions, were sensitive to depth structure and not to position in depth, while a posterior IPS region, the ventral IPS (VIPS) region, had a mixed sensitivity. All three IPS regions were also sensitive to 2D shape, indicating that they carry full 3D shape information. Finally DIPSM, but not DIPSA was sensitive to a saccade-related task. These results underscore the importance of anterior IPS regions in the processing of 3D shape, in agreement with their proximity to grasping-related regions. Moreover, comparison with the results of Durand, J.B., Nelissen, K., Joly, O., Wardak, C., Todd, J.T., Norman, J.F., Janssen, P., Vanduffel, W., Orban, G.A., 2007. Anterior Regions of Monkey Parietal Cortex Process Visual 3D Shape. Neuron 55, 493–505 obtained in the monkey indicates that DIPSA and DIPSM may represent human homologues for the posterior part of AIP and the adjoining part of LIP respectively.

Introduction

The human parietal cortex is thought to extract three-dimensional (3D) shape representations that can support the ability to manipulate objects both physically (Binkofski et al., 1998; Culham et al., 2003) and mentally (Gauthier et al., 2002). 3D shape can be recovered from binocular disparity, which is allegedly the strongest depth cue, yet little is known about the implication of the human parietal cortex in this process. So far, only a couple of studies (Chandrasekaran et al., 2007; Georgieva et al., 2009) have been devoted to the processing of 3D shape from disparity in the human brain. This stands in sharp contrast to the many studies of simple depth from disparity processing which has received much more attention (Backus et al., 2001; Neri et al., 2004; Preston et al., 2008; Tsao et al., 2003; Tyler et al., 2006). Using textured surfaces curved in depth and an interaction design, Georgieva et al. (2009) found several intraparietal sulcus (IPS) regions to be involved in the extraction of depth structure from stereo: the dorsal IPS anterior (DIPSA), the dorsal IPS medial (DIPSM), the parieto-occipital IPS (POIPS) and ventral IPS (VIPS) regions. Interest-ingly, these regions had been previously shown to be involved in the extraction of 3D shape from motion (Murray et al., 2003; Orban et al., 1999; Vanduffel et al., 2002) and also from texture (Georgieva et al., 2008; Shikata et al., 2003; Shikata et al., 2008).

The objective of the present study was to further characterize the role of human parietal cortex in the extraction of 3D shape from disparity. To do that, we used connected random lines as stimuli for the fMRI experiment instead of textured surfaces. Indeed, computational studies (Li and Zucker, 2006a, b) have shown that the processing of both kinds of stereoscopic stimuli requires different operations, and may thus involve different cortical areas. Some support for this view was provided by a recent imaging study in the monkey (Durand et al., 2007). These authors observed that the anterior part of monkey IPS, including posterior AIP and anterior LIP, was involved in processing depth structure from disparity for both textured surfaces and random lines. On the other hand, posterior IPS, corresponding to CIP (Taira et al., 2000; Tsutsui et al., 2002) or pIPS (Denys et al., 2004) or LOP (Lewis and Van Essen, 2000b), was involved chiefly in the extraction of 3D shape from disparity in random lines. Further differences in the activation pattern elicited by the two stimulus sets were observed in ventral premotor cortex and in anterior STS, both of which were activated by 3D shape from disparity in textured surfaces but not in random lines (Durand et al., 2006; Joly et al., 2007). Hence we followed the strategy of Georgieva et al. (2009)

* Corresponding author.
  E-mail address: Guy.Orban@med.kuleuven.be (G.A. Orban).
[1] Present address: Centre de Recherche Cerveau et Cognition, UMR 5549, CNRS-UPS, Toulouse, France.

and used exactly the same random-line stimuli as those used by Durand et al. (2007) in the monkey. This allows us to make two predictions with respect to processing of 3D shape from disparity in human parietal cortex. First, we expect an activation corresponding to anterior IPS in the monkey. Given the earlier hypothesis of Orban et al. (2006) that human regions DIPSM and DIPSA correspond to anterior LIP and posterior AIP in the monkey respectively, we expect an involvement of DIPSM and DIPSA in 3D shape from disparity in random lines, as Georgieva et al. (2009) observed for textured surfaces. Second, in posterior IPS, we expect an additional region to be involved. The homology of monkey CIP/pIPS/LOP is less clear (Shikata et al., 2003; Shikata et al., 2008; Tsao et al., 2003), but one indication from the monkey study (Durand et al., 2007) is that such posterior IPS region should exhibit a mixed sensitivity, being involved in the processing of 3D shape as well as of simple depth from disparity.

There is growing evidence from monkey studies that the two components of the anterior IPS region involved in 2D and 3D shape processing, anterior LIP and posterior AIP, have different single cell properties (Janssen et al., 2008; Lehky and Sereno, 2007; Murata et al., 2000; Sereno and Maunsell, 1998; Srivastava et al., 2006, 2007). This is not surprising, as LIP and AIP are supposedly involved in the control of different effectors: the control of the hand in grasping and manipulation for AIP and the control of the eye and attention for LIP (Andersen et al., 1990; Gnadt and Andersen, 1988; Gottlieb et al., 1998; Murata et al., 2000; Sakata et al., 1995; Snyder et al., 1997; Taira et al., 1990). It is therefore important to distinguish between these two regions and one obvious difference is the activation by saccades, which has been used as an indicator of LIP/AIP boundary (Borra et al., 2008; Luppino et al., 1999). Indeed, imaging studies in monkeys (Baker et al., 2006; Koyama et al., 2004) have shown that LIP is activated by saccades, and Durand et al. (2007) showed that the anterior limit of the saccade activation in IPS corresponds closely to the boundary between LIP and AIP. Therefore the present study used exactly the same saccade task as the Durand et al. study and made the additional prediction, derived from the Orban et al. (2006) hypothesis, that in humans DIPSM, but not DIPSA should be activated in the saccade task.

Thus, in the present experiments we scanned a large group of human subjects with established stereo vision and submitted them to three experiments that were the exact replications of those performed by Durand et al. (2007) in the monkey. First we scanned subjects as they tracked the orientation of a small bar in the fixation plane while we presented the random-line stimuli portraying either a 3D structure, a 2D structure in different depth planes or a 2D structure in the fixation plane. The fixation task ensures that the eyes remain converged on the fixation plane, while we investigated the processing of depth structure from disparity. In a second experiment we tested the subjects with the intact and scrambled images of objects (Denys et al., 2004; Kourtzi and Kanwisher, 2000) to assess sensitivity to 2D shape. In this experiment, subjects fixated a small target while the stimuli were presented, as did the monkeys in the Durand et al. (2007) study. However, an earlier study performed in both species with the same stimuli has shown that introducing a task similar to that used in the first experiment yielded equivalent results (Denys et al., 2004). Regions activated in common in these two experiments are sensitive to both 2D shape and depth structure and can therefore be considered to be involved in the processing of the full 3D shape of objects. Finally, in a third experiment subjects performed the saccade task of Durand et al. (2007).

While the main objectives of the present study were related to the 3D shape processing in human parietal cortex, they also provide additional information about possible homologies between human and monkey parietal cortex. This topic has received considerable interest recently (Binkofski et al., 1998; Bremmer et al., 2001; Culham and Valyear, 2006; Grefkes and Fink, 2005; Grefkes et al., 2002; Hagler et al., 2007; Koyama et al., 2004; Orban et al., 2006; Sereno et al., 2001; Simon et al., 2002; Tsao et al., 2003). Unlike previous studies however, this is the first time that multiple functional tests are compared using parallel imaging of both species. Earlier parallel imaging studies (Denys et al., 2004; Koyama et al., 2004; Sawamura et al., 2005; Tsao et al., 2003; Vanduffel et al., 2002) concentrated on a single functional property: 3D shape from motion, position in depth, saccades, 2D shape processing or adaptation.

Materials and methods

Subjects

Twenty-seven right-handed subjects (including fourteen females, mean age 22 years, range 19–31 years) with normal or corrected-to-normal vision and no history of neurological or psychiatric disease participated in at least one of the three experiments of the present study (see Experimental designs). We ensured that all the subjects involved in the first experiment perceived stereoscopic depth with the stereo stimuli used in this experiment (on this basis, we excluded two subjects who reported weak and unstable stereoscopic percepts). The Ethical Committee of the K.U. Leuven Medical School approved the study, and subjects gave their written informed consent, in accordance with the Helsinki Declaration. Subjects were immobilized in the bore of the horizontal magnet using an individually molded bite-bar. The movements of one eye were monitored during scanning at 60 Hz using a MR-compatible infrared eye-tracking device (ASL eye-tracking system LRO 5000, Applied Science Laboratories, Bedford, USA). Visual stimuli were projected from a liquid crystal display projector (Barco Reality 6400i, 1024 × 768, 60 Hz refresh frequency) onto a translucent screen positioned in the bore of the magnet at a distance of 36 cm from the point of observation. Subjects viewed the stimuli through a mirror attached to the head coil and tilted at 45°.

Experimental designs

We performed three experiments, identical to those performed in the previous fMRI study with behaving macaques (Durand et al., 2007), in order to identify the regions sensitive to shape- and/or position-related information extracted from disparity (first experiment), those sensitive to 2D shape (second experiment), and those involved in ocular saccades (third experiment).

First experiment: sensitivity to visual shape and position along the third dimension

Twenty subjects were included in the first experiment. Stimuli (Fig. 1) were red/green anaglyphs of connected random-line patterns (9 to 12 segments subtending an average visual angle of 9°; segment width = 0.05° and length = 0.5 to 9°). In the low-level condition, the images for both eyes were always identical ('Zero disparity') and stimuli were perceived as 2D random-line patterns located in the fixation plane. In the other two conditions, binocular disparity was introduced and stimuli were perceived either as 3D patterns centered on the fixation plane ('3D structure') or as 2D patterns located either in front, behind or in the fixation plane ('3D position'). During scanning, stimuli were presented in 30 s blocks in which different stimuli of a given condition were shown successively, each for 3 s. Successive stimuli portrayed different structures or positions in depth (in the conditions '3D structure' and '3D position' respectively) in order (1) to avoid adaptation to the disparity signal and (2) to recruit larger populations of neurons tuned to different structures and/or positions in depth. Note that neurons tuned to position in depth should respond to the condition 'Zero disparity', because a null disparity indicates a particular stimulus location: the fixation plane. However, stronger activations are expected in the '3D position'
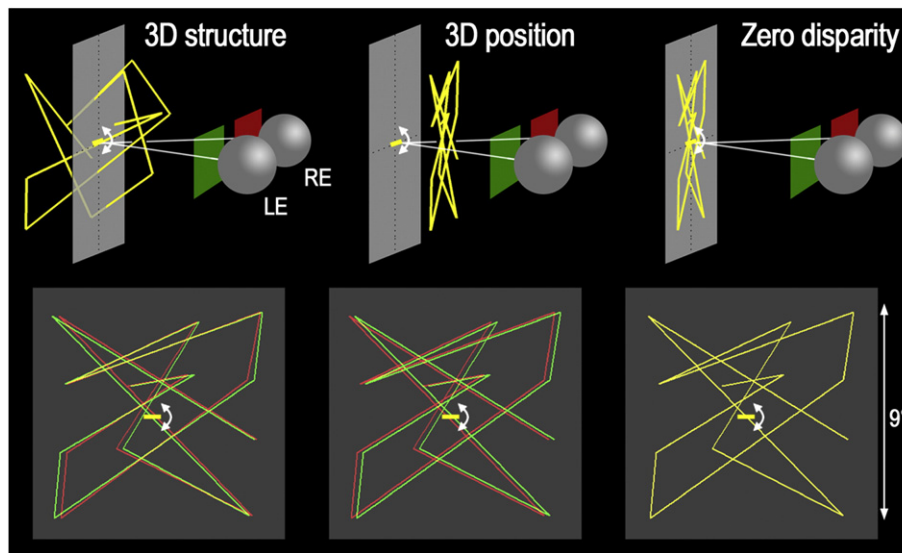
Fig. 1. Visual stimuli in the first experiment. Stimuli were red/green anaglyphs of connected segments forming random patterns (lower row). As illustrated in the upper row, binocular disparity specified 3D patterns of random lines centered on the fixation target in the condition '3D structure', and fronto-parallel patterns of random lines that could appear in front, behind or at the fixation plane (i.e. the screen) in the condition '3D position'. In the condition 'Zero disparity', similar images were presented to both eyes, so that the stimuli were perceived as fronto-parallel random-line patterns systematically positioned in the fixation plane. During scanning, subjects had to report sudden changes in the orientation of a small fixation bar. Note that the images seen by both eyes were well segregated by the colored filters of the stereo glasses, with a moderate cross talk of 15%. None of the subjects reported seeing 'ghost images', as can arise when the two monocular images are poorly segregated.

condition for two reasons. First, the range of stimulus positions encompasses the fixation plane, so that neurons tuned to stimuli at, but also in front or behind the fixation plane should be recruited. Second, adaptation to a constant disparity signal is likely to occur in the condition 'Zero disparity', but is prevented in the condition '3D position' by varying the position in depth of successive stimuli.

In the macaque study (Durand et al., 2007), a new and unique random-line pattern was generated online for each stimulus presentation, so that a large number of stimulus presentations was required to equalize the monocular properties of the stimuli across conditions. In the present study, human subjects were scanned for shorter durations, and we could not present such a large number of stimuli to the subjects. Thus, we generated the stimuli for the conditions '3D structure', '3D position' and 'Zero disparity' from identical monocular random-dot patterns (an example is shown in Fig. 1). That way, we insured that the monocular properties of the stimuli (and possible monocular depth cues such as segment intersections and angles made by the segment junctions) were balanced between visual conditions despite the smaller number of stimulus presentations per subject.

Regions processing depth from binocular disparity were identified by comparing the activations elicited by stimuli in which binocular disparity was manipulated to those produced by similar stimuli with zero disparity ('3D structure and 3D position'>twice 'Zero disparity'). We further distinguished the regions preferentially engaged in processing shape-related information or depth structure ('3D structure'>'3D position') and those activated by position in depth ('3D position'>'Zero disparity').

We checked that all participants could easily perceived stereoscopic depth in a representative subset of the random-line stimuli by asking them to describe verbally the depth structure and position in depth of the stimuli presented in the scanner (before scanning). Thus, we insured that all the subjects could perceive effortlessly the stereo-disparity introduced experimentally, even if we did not measure their stereo threshold. On this basis, two subjects were rejected for weak or unstable stereoscopic vision. During scanning, subjects performed a high-acuity fixation task (Sawamura et al., 2005; Vanduffel et al., 2002). They were required to interrupt an infrared beam with the

index finger following sudden orientation changes (from horizontal to vertical) of a small yellow fixation bar in the center of the display. Subjects performed a preliminary session in the scanner to determine the bar size yielding about 80% correct responses ($0.15° \times 0.05°$ for 6 subjects, $0.20° \times 0.05°$ for 12 subjects and $0.25° \times 0.05°$ for 2 subjects). This task recruits the attentional resources of the subjects and forces them to gaze accurately at the fixation target, minimizing both differences in attention paid to 3D *versus* 2D stimuli and disparity-driven eye movements (Boltz and Harwerth, 1979).

Second experiment: Visual shape sensitivity in the fronto-parallel plane

Seventeen of the subjects involved in the first experiment participated in the second experiment. Stimuli were intact and scrambled versions of both grayscale images and line drawings of familiar objects (Denys et al., 2004; Kourtzi and Kanwisher, 2000) measuring $12° \times 12°$ and displayed in the center of the screen. Line drawings were obtained by tracing the outer and inner contours of the grayscale images, and scrambling was achieved by placing a 20×20 grid over the intact stimuli and by shuffling the positions of the resulting squares. Eight different stimuli from the same condition were shown successively (for 3 s each) during blocks of visual conditions. The regions processing 2D shape were identified by the main effect of scrambling ('Intact'>'Scrambled'). In keeping with our previous monkey study, subjects had to fixate a small target that was continuously visible at the center of the screen. A conjunction analysis between the results of the first and second experiment was used to identify the regions sensitive to visual 3D shape, i.e. the regions processing visual shape both along the third dimension (depth structure) and in the 2D fronto-parallel plane. Conjunction analyses (Prize and Friston, 1997; Friston et al., 1999) are used to find regions that are active in a number of tasks targeting the same cognitive process, i.e. regions that are involved in this process independently of a particular task. In the present study, this analysis was performed to find regions processing visual shape, independently of whether the subtraction targeted shape sensitivity along the depth dimension ('3D shape'>'3D position' in the first experiment) or in the fronto-parallel plane ('Intact'>'Scrambled' in the second experiment).

Third experiment: Sensitivity to saccadic eye movements

Fourteen subjects (seven of whom participated in the two other experiments) were recruited. In the 'Saccade' condition, subjects had to saccade toward a red visual target ($0.1° \times 0.1°$) jumping pseudo-randomly, every 3 s, among three locations along the horizontal meridian (0° or $\pm 7°$). In the 'Visual control' condition, subjects had to hold their fixation on a central fixation target (0°) while visual distractors were successively flashed for 300 ms, with 2.7 s intervals, at 7° or 14° of eccentricity, either to the left or to the right of the fixation target. Both the direction and the eccentricity of the visual distractors were matched with those of the visual target in the saccade condition (1/2 left and 1/2 right; 2/3 at 7° and 1/3 at 14°). Regions involved in ocular saccades were identified by the contrast 'Saccade'>'Visual control'.

A block design was used in all three experiments. Time series of 120 functional volumes consisted of successive blocks of 8 to 10 functional volumes (24 to 30 s), corresponding to the different experimental conditions. All the experiments contained a baseline condition during which the fixation target was presented with no stimulus in the background. The condition order was pseudo-randomized between the time series. For each subject, we acquired 6 time series in the first experiment, and 2 time series in the second and third experiments. In addition, we acquired a motion localizer (2 time series) for the seventeen subjects involved in the first and second experiments. Stimuli were circular random-dot patterns (dot size = 0.01°; density = 50%) covering 14° of visual angle. To identify the motion sensitive regions, conditions in which the stimuli translated at a speed of 4°/s, in one of 8 directions (4 cardinal and 4 oblique), were contrasted with conditions in which they were static (Sunaert et al., 1999).

Data collection

Data were collected with a 3 T MR scanner (Intera, Philips Medical Systems, Best, The Netherlands). Functional volumes were gradient-echoplanar, whole-brain images (50 horizontal slices; slice thickness/gap 2.5/0.25 mm; 80×80 acquisition matrix with in-plane resolution 2.5×2.5 mm; TR/TE 3000/30 ms). A high-resolution T1-weighted image covering the entire brain was acquired between the third and fourth time series of the first experiment (or at the end of the third experiment for the seven subjects involved in only this experiment) to use as anatomical reference (182 coronal slices; slice thickness 1.2 mm; 256/256 acquisition matrix with in-plane resolution 1×1 mm; TR/TE/TI 9.7/4.6/900 ms).

Data analysis

Functional image analysis

fMRI data were analyzed with SPM5 software (Wellcome Department of Imaging Neurosciences, University College London, U.K., http://www.fil.ion.ucl.ac.uk/spm) implemented on MATLAB (Mathworks, Inc., Natick, MA). The pre-processing steps included realignment, coregistration of the anatomical images to the functional scans, and spatial normalization into standard MNI space. The functional data were sub-sampled in the normalization step to $2 \times 2 \times 2$ mm voxels and then smoothed with an isotropic Gaussian kernel (full width at half-max: 6 mm).

Statistical analyses were performed using the General Linear Model (GLM) with a fixed-effect approach in single subjects and a random-effect approach in the groups. In all the analyses, the statistical threshold was set at $p < 0.05$ with a false discovery rate (FDR) correction for multiple comparisons (Genovese et al., 2002) and, in the first and second experiments, the statistical maps were masked inclusively with the visually-active voxels ('Stimulus conditions'>'Fixation baseline'; $p < 0.05$ with FDR correction). We used a classical ANOVA model (repeated measure) for the random-effect analyses, except in the first experiment where an ANCOVA model was chosen to include differences in performance in the high-acuity task as a nuisance variable. We ensured that an ANOVA design excluding those subjects showing significant interactions between performance and visual conditions produced similar results. We compared the results of random-effect analyses obtained by ANCOVA (with all subjects) and ANOVA (after excluding those subjects who showed a significant interaction between behavioral performance and visual conditions) in two ways. We first correlated the non-thresholded contrast images produced by the two models (as computed by SPM5), retaining all the visually-active voxels ($p < 0.05$, FDR correction). Then, to assess the spatial reproducibility of the significant activations, we computed a percentage of overlap between thresholded activations ($p < 0.05$, FDR correction) as follows: $P_{overlap} = (2 \times V_{1,2}) / (V_1 + V_2) \times 100$; where V_1, V_2 and $V_{1,2}$ are the numbers of active voxels in the first, in the second, and common to both estimates of a given contrast (Rombouts et al., 1998). For the conjunction analysis targeting 3D shape sensitivity, only the 17 subjects common to the first two experiments were used. The conjunction was performed by entering the individual contrast images obtained in the subtractions '3D structure'>'3D position' (first experiment) and 'Intact'>'Scrambled' (second experiment) in a t-test design, and calculating the conjunction null hypothesis with SPM5 between these two groups of contrast images. The conjunction returns a t-score map indicating the probability that voxels are significantly activated in both subtractions at the group level.

To assess the robustness and the generality of the results obtained at the group level, single-subject analyses were used in the following manner: whole-brain images were constructed in which the value of each voxel reflected the percentage of subjects showing significant activation ($p < 0.05$ FDR corrected) at that particular location.

Data visualization

We used Caret (Van Essen et al., 2001; http://brainvis.wustl.edu/caret/) to project the t-score maps and the percentage maps constructed from single-subject analyses (see Data analysis) onto a surface from the human Population Averaged Landmark and Surface (PALS) atlas (Van Essen, 2005; http://sumsdb.wustl.edu:8081/sums/directory.do?id=636032). Retinotopic borders (Van Essen, 2004) of areas V1, V2 and V3 were superimposed onto the maps.

Eye movement analysis

Eye movement traces were analyzed to ensure (1) that the quality of fixation did not differ among the different stimulus conditions in the first and second experiments and (2) that subjects performed the saccade task correctly in the third experiment. Traces were high-pass filtered (>0.1 Hz) to correct for drifts and parts of the traces associated with high-frequency noise, i.e. eye velocities exceeding 600°/s (Becker, 1989), were discarded. In the first and second experiments, saccades were detected as the parts of the traces associated with eye velocity >20°/s and with eye positions at least one standard deviation away from the mean eye position (at fixation) in the horizontal and/or vertical dimension. Neither the mean numbers of saccades per minute (9.14 and 8.98 averaged across conditions of experiments 1 and 2 respectively) nor the mean standard deviations (2.09° and 2.42° horizontally, 1.98° and 2.20° vertically) differed significantly (Wilcoxon rank-sum test) between the stimulus conditions for any of the subjects in either experiment. In the third experiment, eye movements were monitored online to check that subjects actually performed the saccade task (Fig. 2). An offline analysis confirmed that subjects performed the task accurately, largely confining their gaze to a fixation window of $\pm 2°$ centered on the visual target both in the 'Visual control' condition (mean: 86.2%; worst subject: 77.0%;
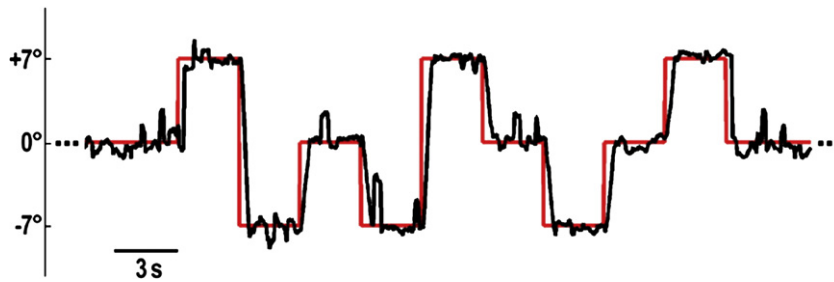
Fig. 2. Example of horizontal eye traces (in black) during a block of saccades for one of the subject involved in the third experiment. The visual target jumps pseudo-randomly every 3 s to occupy one of three locations along the horizontal meridian: $-7°$ (left), $0°$ (center) or $+7°$ (right). The actual location of the visual target is shown in red.

best subject: 95.4%) and in the 'Saccade' condition (mean: 84.6%; worst subject: 76.1%; best subject: 94.7%).

Results

Sensitivity to depth structure extracted from disparity (first experiment)

In the first experiment, we identified, amongst the cortical regions sensitive to binocular disparity ('3D structure and 3D position'>twice 'Zero disparity'), those sensitive to shape-related information or depth structure ('3D structure'>'3D position') and those sensitive to position in depth ('3D position'>'Zero disparity'). Fig. 3 shows the performances in the acuity task for the 20 subjects during scanning. Percentage of correct detections averaged 83.8% across the subjects and ranged from 73.6% to 91.4%. Five of the 20 subjects exhibited a slight but significant ($p<0.05$, Wilcoxon rank-sum test) drop in performance in the condition '3D position' (from 4.2% to 7.2% relative to the condition '3D structure'). For this reason we used an ANCOVA model for analysis taking the behavioral performance as a nuisance factor. The results obtained with this model for the group of twenty human subjects are shown in Fig. 4A (random-effect analysis, $p<0.05$ with FDR correction). The regions sensitive to binocular disparity, those preferentially activated by shape-related information and those responding to position-related information are color coded in white, red and yellow respectively and are overlaid onto flattened representations of the left and right cortical hemispheres (PALS atlas). Regions responding preferentially to shape-related information but also activated by position-related disparity information are color coded in orange.

The cortical network processing binocular disparity (in white) is broadly distributed, encompassing extra-striate visual areas and higher-order areas in both the dorsal and ventral visual streams. In the ventral stream, the activation sites include the different parts of the lateral occipital complex (LOC): the lateral occipital sulcus (LOS), the posterior infero-temporal gyrus (post-ITG), and the middle fusiform gyrus (Mid-FG) as described by Denys et al. (2004). In the dorsal stream, activations are found in the MT/V5 complex (defined by the motion localizer) and over the whole extent of the IPS, from the transverse occipital sulcus (TOS) to the posterior bank of the post-central sulcus (post-CS). The dorsal activation also encompasses the anterior part of the parieto-occipital sulcus (POS) and the superior parietal lobule.

Within this cortical network, the regions more sensitive to depth structure (in red and orange) include early extra-striate areas, the LOS, the posterior part of the MT/V5 complex, and both the anterior and posterior parts of the IPS (aIPS and pIPS). Those processing position in depth (in yellow and orange) are located ventrally in the post-ITG and Mid-FG (for related results, see Gilaie-Dotan et al., 2002; Kourtzi et al., 2003; Preston et al., 2008). In the dorsal stream, activations are found in the anterior part of the MT/V5 complex, in the anterior part of the POS (a location that could house the homologue of area V6 in monkeys; Pitzalis et al., 2006) and in the intermediate and posterior parts of the IPS (iIPS and pIPS). Sensitivity to position in depth in these parietal regions has already been reported for stereoscopic surfaces (Neri et al., 2004; Preston et al., 2008; Tsao et al. 2003), and it could be inherited from V3A (Backus et al., 2001). Our design does not allow us to disentangle whether these regions are driven by absolute retinal disparity (with respect to the fovea) or by relative disparity (with
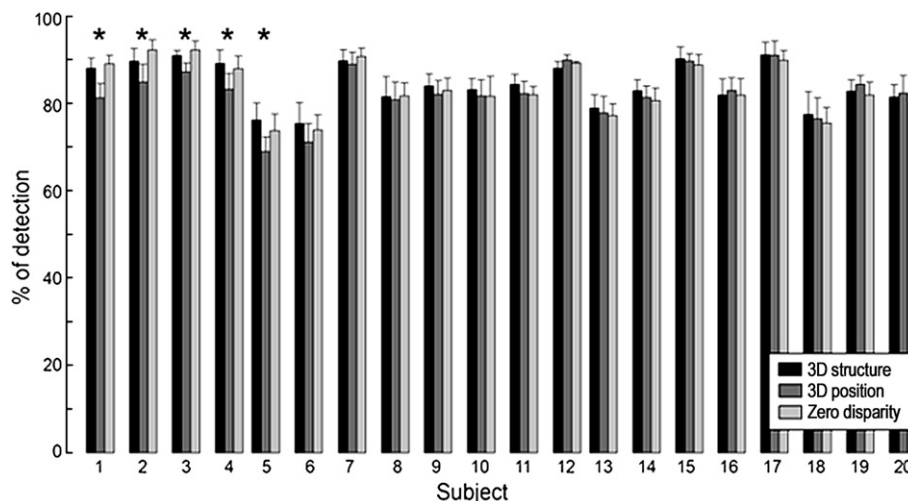
Fig. 3. Performance levels in the high-acuity fixation task of the first experiment. Percentages of correct detections are plotted for the different subjects and stimulus conditions. Asterisks indicate a significant drop in performance in the condition '3D position' (*$p<0.05$, Wilcoxon rank-sum test).
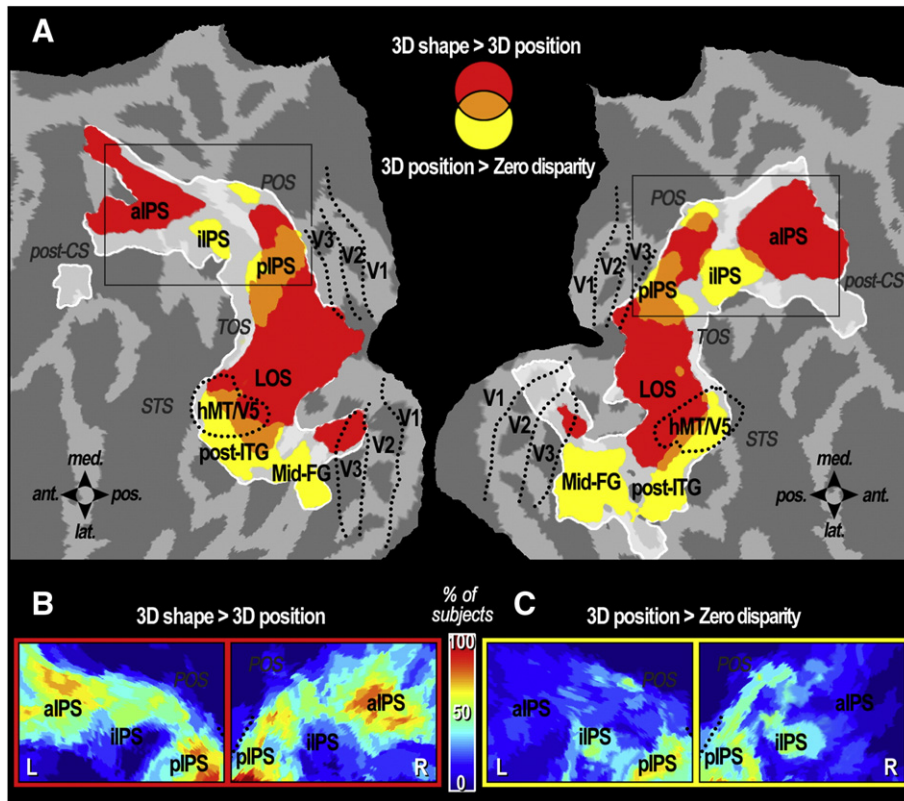
Fig. 4. (A) Results of the first experiment (random-effect analysis, ANCOVA model, $n = 20$ subjects, $p < 0.05$, FDR correction for multiple comparisons) projected onto flattened representations of the left and right cortical hemispheres (PALS atlas; posterior part only). White outlines show the regions activated by binocular disparity. Red, yellow and orange color-codes respectively indicate the regions more sensitive to shape-related information or depth structure ('3D structure'>'3D position'), those sensitive to position in depth ('3D position'>'Zero disparity') and those exhibiting both properties. Black dotted lines show the retinotopic borders of areas V1, V2 and V3 (taken from Caret) and the hMT/V5 complex as revealed by the motion localizer experiment (t-score>8). (a/i/p IPS: anterior/intermediate/posterior intraparietal sulcus, mid-FG: middle fusiform gyrus, post-CS: post-central sulcus, post-ITG: posterior inferior temporal gyrus, STS: superior temporal sulcus, TOS: transverse occipital sulcus). (B, C) Percentage of individual subjects showing significant activations (fixed-effect analysis, $p < 0.05$, FDR correction for multiple comparisons) around aIPS (black rectangle in A) for the contrasts '3D structure'>'3D position' and '3D position'>'Zero disparity' respectively (L/R: left and right hemispheres).

respect to the small fixation bar), but an earlier human fMRI study indicates that position in depth sensitivity may rely mainly on absolute disparity in the dorsal stream (Neri et al., 2004). Interestingly, this signal is suited for ocular saccades in 3D space, and neurons tuned to absolute disparity have been described in macaque LIP (Gnadt and Mays, 1995).

Thus, it appears that in humans, as predicted, two regions in the IPS, an anterior and a posterior one are sensitive to depth structure defined by disparity. The anterior intraparietal sulcus (aIPS) is sensitive to binocular disparity when this signal defines depth structure, but not to the position in depth of visual stimuli, whereas the posterior site (pIPS) has a mixed sensitivity.

These results were obtained with an ANCOVA model. However, a more standard ANOVA model yielded very similar results after excluding the five subjects showing interactions between performance and visual conditions (Fig. 5). Voxel-based correlation coefficients (r) of 0.94 and 0.91 were found for the contrast images respectively targeting depth structure and position in depth in the two models, indicating that these two models produce very similar activation patterns. Furthermore, the significant activations yielded by the two models produced a $P_{overlap}$ of 88% and 80% for the contrasts targeting depth structure and position in depth respectively, allowing us to conclude that our results do not depend specifically on the use of an ANCOVA model.

To further assess the consistency of these results at the level of individual subjects, Fig. 4B and C show the percentages of individual subjects showing significant activation (fixed-effect analysis, $p < 0.05$ with FDR correction) in the IPS (black rectangle in Fig. 4A) for the

contrasts '3D structure'>'3D position' and '3D position'>'Zero disparity', respectively. These maps indicate that the former contrast is consistently associated with significant activations at the level of aIPS and pIPS in the majority of the individual subjects. On the other hand in about half the subjects the latter contrast is associated with activation of pIPS. Together, these analyses demonstrate that aIPS is sensitive to the depth structure of visual stimuli but does not respond to their position in depth, while pIPS is sensitive to both aspects.

Visual 2D shape sensitivity (second experiment) and conjunction analysis between depth structure and 2D shape sensitivity (first and second experiments)

In the second experiment, we addressed visual 2D shape sensitivity by visualizing the regions more active for intact than for scrambled images of objects. As shown in Fig. 6 (blue areas) for the group of 17 subjects (random-effect analysis, $p < 0.05$ with FDR correction), 2D shape processing engages a large cortical network encompassing both the ventral and dorsal visual streams. Notably, we found significant activations within the human parietal cortex, as previously documented using identical stimuli (Denys et al., 2004).

Regions in which shape sensitivity along the depth dimension (in red) and in the fronto-parallel plane (in blue) actually converged were identified by a conjunction analysis across the 17 subjects who were tested for both properties (random-effect analysis, $p < 0.05$ with FDR correction). These regions, which can be considered as sensitive to 3D shape defined by disparity, are shown in Fig. 6A by the hot color map. They include the anterior and posterior parts of the IPS, but also the
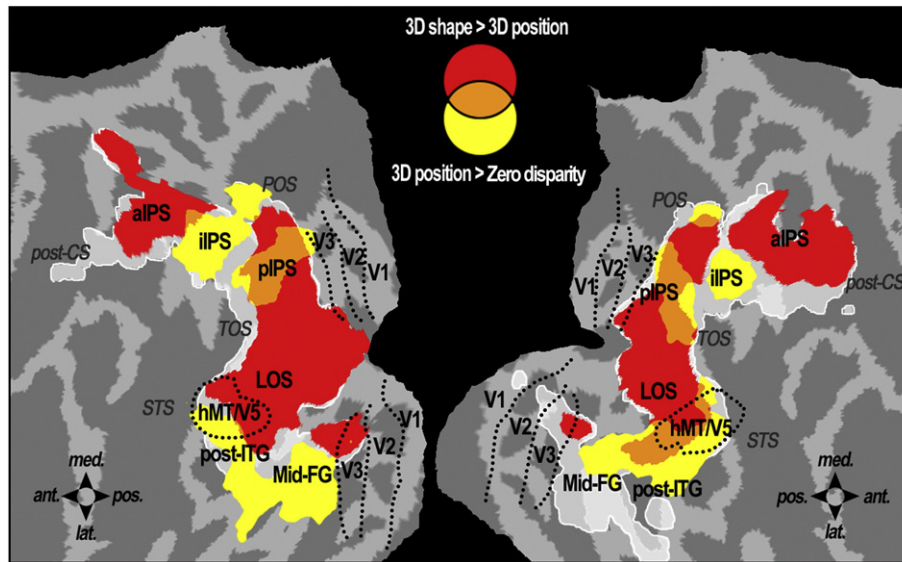
Fig. 5. Results of the first experiment for the 15 subjects showing no difference in task performance across visual conditions (random-effect analysis, ANOVA model, *p*<0.05, FDR correction for multiple comparisons). Same conventions as Fig. 4A.

LOS and the posterior part of the hMT/V5 complex, in agreement with earlier indications of shape sensitivity in those regions (Brouwer et al., 2005; Chandrasekaran et al., 2007; Kourtzi et al., 2003; Orban et al., 1999; Welchman et al., 2005).

The white embossed circular symbols in Fig. 6A represent the statistical local maxima found in the parietal cortex with the conjunction analysis, listed in Table 1. These three maxima were close to those obtained in the first two experiments separately and
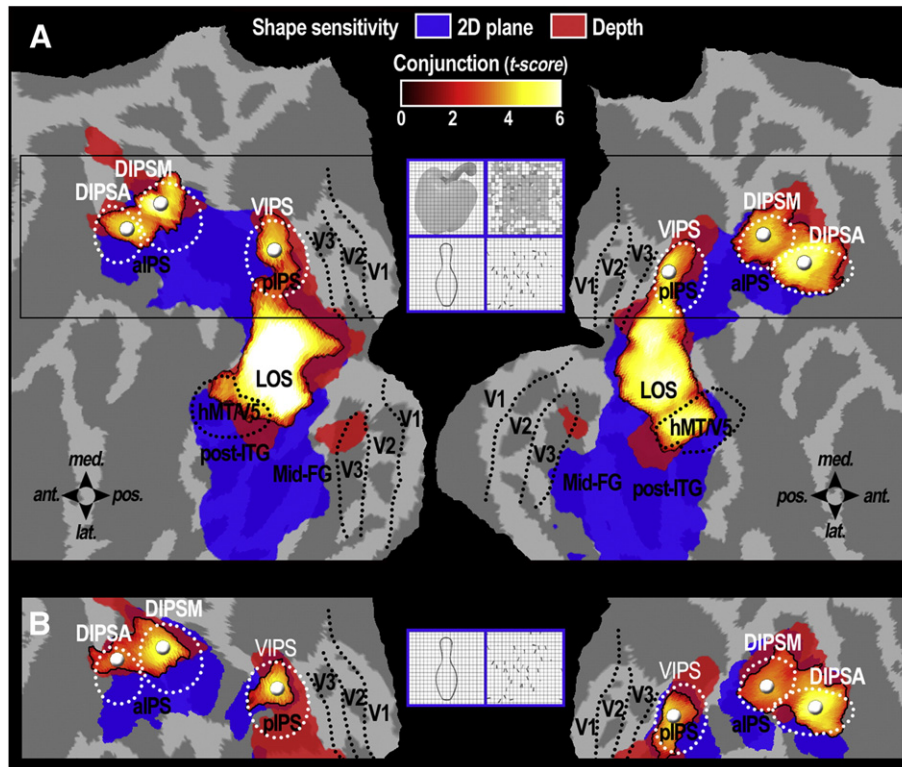
Fig. 6. (A) Results of the conjunction analysis between the first and second experiments (random-effect analysis, *n* = 17 subjects, *p*<0.05, FDR correction for multiple comparisons) projected onto flattened representations of the left and right cortical hemispheres (PALS atlas; posterior part only). Examples of grayscale images and line-drawing stimuli (intact and scrambled versions) used in the second experiment are shown between the left and right hemispheres. Blue and red areas indicate the regions sensitive to shape-related information in the 2D retinal plane (second experiment) and along the depth dimension (first experiment) respectively. Regions processing visual 3D shape were thus revealed by a conjunction analysis across the 17 subjects tested in both experiments (hot color map). White embossed circular symbols show the location of the local maxima for the conjunction analysis in anterior IPS: DIPSA and DIPSM (anterior and medial parts of the dorsal IPS) and in posterior IPS: VIPS (ventral IPS). White dotted ellipses around these local maxima represent confidence intervals based on previous studies (Claeys et al., 2003; Denys et al., 2004; Orban et al., 2006; Orban et al., 2003; Orban et al., 1999). (B) Same as (A) except that 2D shape sensitivity was assessed solely with line-drawing stimuli (grayscale images excluded).

Table 1
MNI coordinates for the parietal local maxima (and corresponding t-scores).

			Conjunction	3D shape>3D position	3D position>No disparity	2D shapeIntact>Scramb.	Motion localizer Motion>Static
pIPS	VIPS	L	−26 −84 34 (5.0)	−24 −82 32 (6.1)	−24 −82 28 (5.1)	−26 −82 30 (10.2)	−20 −86 26 (6.4)
		R	26 −82 32 (5.3)	24 −86 30 (5.7)	22 −84 32 (4.0)	26 −84 34 (9.8)	28 −80 34 (6.6)
aIPS	DIPSM	L	−24 −62 60 (6.5)	−22 −62 56 (7.0)		−26 −62 62 (8.9)	−20 −60 64 (8.2)
		R	26 −64 64 (5.2)	24 −64 58 (7.4)		24 −62 54 (11.5)	24 −62 60 (8.7)
	DIPSA	L	−30 −54 64 (4.9)	−30 −50 64 (5.8)		−34 −48 60 (10.4)	−30 −52 60 (7.8)
		R	32 −50 62 (6.2)	34 −48 62 (5.3)		36 −52 58 (9.4)	32 −50 66 (6.3)

Threshold t-scores for FDR corrected $p<0.05$ ranged from $t=2.4$ to 2.7 in the different subtractions; threshold t-scores for FWE corrected $p<0.05$ equaled 5.3 for the conjunction and the random-line subtractions, 6.6 for the shape localizer and 5.9 for the motion localizer.

with the motion localizer (Table 1). This proximity indicates that the parietal regions processing visual 3D shape from disparity and those sensitive to 2D and 3D motion (Orban et al., 1999; Sunaert et al., 1999) are likely to be the same. This was confirmed by the fact that confidence intervals (white dotted ellipses in Fig. 6) drawn from local maxima reported in previous studies on motion sensitivity (Claeys et al., 2003; Denys et al., 2004; Orban et al., 2006, 2003, 1999) encompass those obtained in the conjunction analysis. We thus named these regions in accordance with the above-mentioned studies: ventral IPS (VIPS), medial and anterior parts of dorsal IPS (DIPSM and DIPSA). These regions, together with their confidence intervals, are shown on inflated representations of both hemispheres in Fig. 8A.

We repeated the conjunction after removing from the analysis the data obtained with grayscale images of objects. Only line-drawing stimuli were retained in order to remove potential confounds due to the presence of monocular depth cues such as shading in grayscale images. As shown in Fig. 6B, the results were qualitatively similar in the parietal cortex (black rectangle in Fig. 6A), indicating that our results are unlikely to be affected by these confounding factors, in
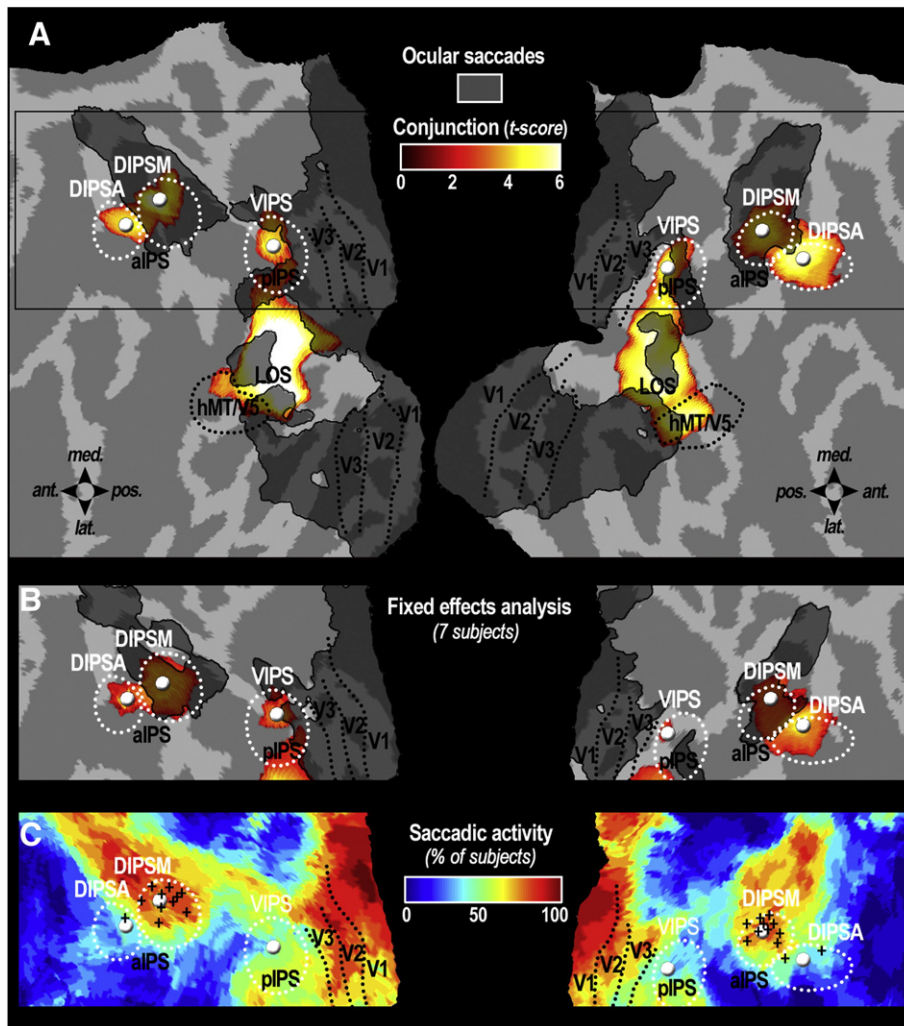
Fig. 7. (A) Results of the third experiment (random-effect analysis, $n = 14$ subjects, $p<0.05$, FDR correction for multiple comparisons) projected onto flattened representations of the left and right cortical hemispheres (PALS atlas; posterior part only). The regions involved in ocular saccades ('Saccade'>'Visual control') are shown in black, overlaid onto the results of the conjunction analysis between shape sensitivity along the depth dimension and in the 2D retinal plane (from Fig. 6A). (B) Same as (A) but with results of the third experiment and conjunction analysis restricted to the 7 subjects involved in all three experiments (fixed-effect analysis, $p<0.05$, FDR correction for multiple comparisons). (C) Percentage of subjects showing significant saccade-related activations (fixed-effect analysis, $p<0.05$, FDR correction for multiple comparisons). Black crosses indicate individual statistical local maxima encountered within the confidence intervals of DIPSM and DIPSA.

agreement with Denys et al. (2004). Also the results of Georgieva et al. (2008) indicate that shading has little effect in human parietal cortex.

Parietal regions involved in ocular saccades (third experiment)

The results of these two experiments and of the conjunction analysis indicate the existence in human parietal cortex of an anterior complex, including two local maxima DIPSM and DIPSA, that is sensitive to visual 3D shape extracted from disparity. The third experiment tests the final predication that these two local maxima can be distinguished by saccade-related activity. Fourteen human subjects participated, of whom 7 subjects were also involved in the first two experiments. Subjects had either to saccade toward a red visual target jumping among three locations ('Saccade'), or to keep their gaze on a central fixation target while visual distractors were flashed ('Visual control'). In Fig. 7A, black areas indicate significant saccade-related activity ('Saccade'>'Visual control', random-effect analysis, $p < 0.05$ with FDR correction) overlaid onto the results of the conjunction analysis targeting visual 3D sensitivity.

The results show that ocular saccades actually elicit activations in DIPSM but not in DIPSA. Statistical local maxima in anterior IPS were encountered in the neighboring of DIPSM in both hemispheres (Left: -18, -60, 58, $t = 9.29$; Right: 20, -62, 58, $t = 10.15$). At the coordinates of DIPSA given by the conjunction analysis (Table 1), t-values were 1.22 and 1.57 for the left and right hemisphere respectively, and both values fail to reach the very permissive statistical threshold of $p < 0.05$ uncorrected for multiple comparisons ($t = 1.78$). Thus, statistical thresholding is not an issue for the functional difference found between DIPSM and DIPSA with the ocular saccade task. In order to insure that this result was not an artifact due to differences in group compositions between the two first experiments and the third, we performed a group analysis restricted to the seven subjects involved in all three experiments (fixed-effect analysis, $p < 0.05$ with FDR correction). As shown in Fig. 7B, this analysis produces qualitatively similar results. First, sensitivity to visual 3D shape is encountered in VIPS, DIPSM and DIPSA in this subpopulation. Second, saccade-related activity sampled from the same subpopulation is found in DIPSM (t-values of 7.79 and 6.98 for the left and right hemispheres respectively) but not in DIPSA (t-values of 1.08 and 1.13). Finally, we assessed the consistency of this result at the level of individual subjects by calculating the percentage of subjects exhibiting significant saccade-related activations (fixed-effect analysis, $p < 0.05$ with FDR correction). As shown in Fig. 7C, about 80% (11/14) of the subjects showed significant saccade-related activations within the confidence interval around DIPSM, and 91% (10/11) of these had local maxima within this region (black crosses in Fig. 7C). Despite the proximity of DIPSM and DIPSA, the saccade-related activations encompassed DIPSA in only 35% (5/14) of the subjects. The fact that 1/3 of the subjects show significant activation within the confidence interval of DIPSA is likely due to the spreading, caused by smoothing, of saccade-related activity from DIPSM, since local maxima around DIPSA were encountered in only 2 subjects (black crosses in Fig. 7C). Thus the proportion of subjects with a local maximum of saccade-related activity in the vicinity of DIPSM (10/14) is significantly larger ($\chi^2 = 9.33$, $p < 0.01$) than in the neighborhood of DIPSA (2/14), despite the definition of the confidence limits around the group coordinates rather than individual coordinates. Overall, these analyses indicate that DIPSM and DIPSA can be differentiated on the basis of activation by ocular saccades, bearing out our final prediction.

Discussion

Our results show that, as predicted, human parietal cortex includes two regions involved in the processing of 3D shape from disparity. The anterior region is sensitive to depth structure but not to position in

depth. It includes two sites DIPSM and DIPSA that differ in their sensitivity to saccades. The second posterior region has a mixed sensitivity and corresponds to VIPS.

Methodological issues

The results were consistent across subjects, as assessed by the single-subjects' analyses, and we took care to exclude confounding factors such as group compositions and quality of fixation. The demanding high-acuity task in the first experiment prevented subjects from devoting more attention to 3D than to 2D stimuli, and forced them to maintain accurate fixation upon the central target. The high-acuity task requires central fixation, including in depth, to be performed correctly. Hence, it is likely that the decrease in performance in the position in depth condition observed in some subjects reflects small vergence eye movements, impossible to measure with eye position recordings of a single eye. However, these slight differences in performances were included as nuisance factor in the ANCOVA analysis to cancel out this potential confound. Further analysis showed that using an ANOVA after excluding those subjects showing an interaction between performance and visual conditions, rather than an ANCOVA, did not influence our results. The second experiment was performed under passive viewing conditions, but the same set of stimuli has been shown to elicit similar parietal activations with a high-acuity task (Denys et al., 2004). Thus neither attention nor eye movements, which are known to activate the parietal cortex (Corbetta and Shulman, 2002; Kanwisher and Wojciulik, 2000; Kourtzi and Kanwisher, 2000), have a significant impact on the results of experiments 1 and 2. Moreover, in the third experiment we ensured that all the subjects performed the ocular saccade task accurately.

Anterior parietal regions

The involvement of DIPSM and DIPSA in processing 3D shape from disparity is in agreement with the recent study of Georgieva et al. (2009) and with the earlier results of Chandrasekaran et al. (2007). These two areas can thus process depth structure both in textured surfaces or in contours, despite the fact that computational studies have shown that extracting depth structure in such stimuli relies on distinct algorithms (Li and Zucker, 2006a, b). Furthermore, the present study is the first to offer a clear functional differentiation between these two regions, which in most previous studies (Denys et al., 2004; Georgieva et al., 2009; Orban et al., 1999; Sunaert et al., 1999; Vanduffel et al., 2002) reacted similarly. In contrast, we have demonstrated that DIPSM is activated by ocular saccades and DIPSA is not. This result was found both for the group and at the level of individual subjects, and it was independent of the statistical threshold used. It will be the aim of future studies to find a task that may engage DIPSA but not DIPSM, in order to provide evidence for a double functional dissociation between these regions. As shown in Fig. 8B, there is an excellent agreement between the saccade-related activity we found in the present study (black areas) and parietal local maxima (purple symbols) reported in previous studies with saccade and/or spatial attention tasks (Astafiev et al., 2003; Connolly et al., 2002; Corbetta et al., 1998; Koyama et al., 2004; Medendorp et al., 2005; Schluppeck et al., 2005; Sereno et al., 2001; Simon et al., 2002; Wojciulik and Kanwisher, 1999). The regions involved in saccade-related task are clearly posterior to those activated by grasping-related tasks, as shown by the green circular symbols in Fig. 8B (Begliomini et al., 2007; Binkofski et al., 1999, 1998; Cavina-Pratesi et al., 2007; Culham et al., 2003; Frey et al., 2005; Kroliczak et al., 2007). These studies consistently reported activations in a location considered to be human AIP (hAIP), which is slightly anterior to DIPSA. The absence of 3D visual shape sensitivity in hAIP in the present study is in agreement with a previous report (Culham et al., 2003). In
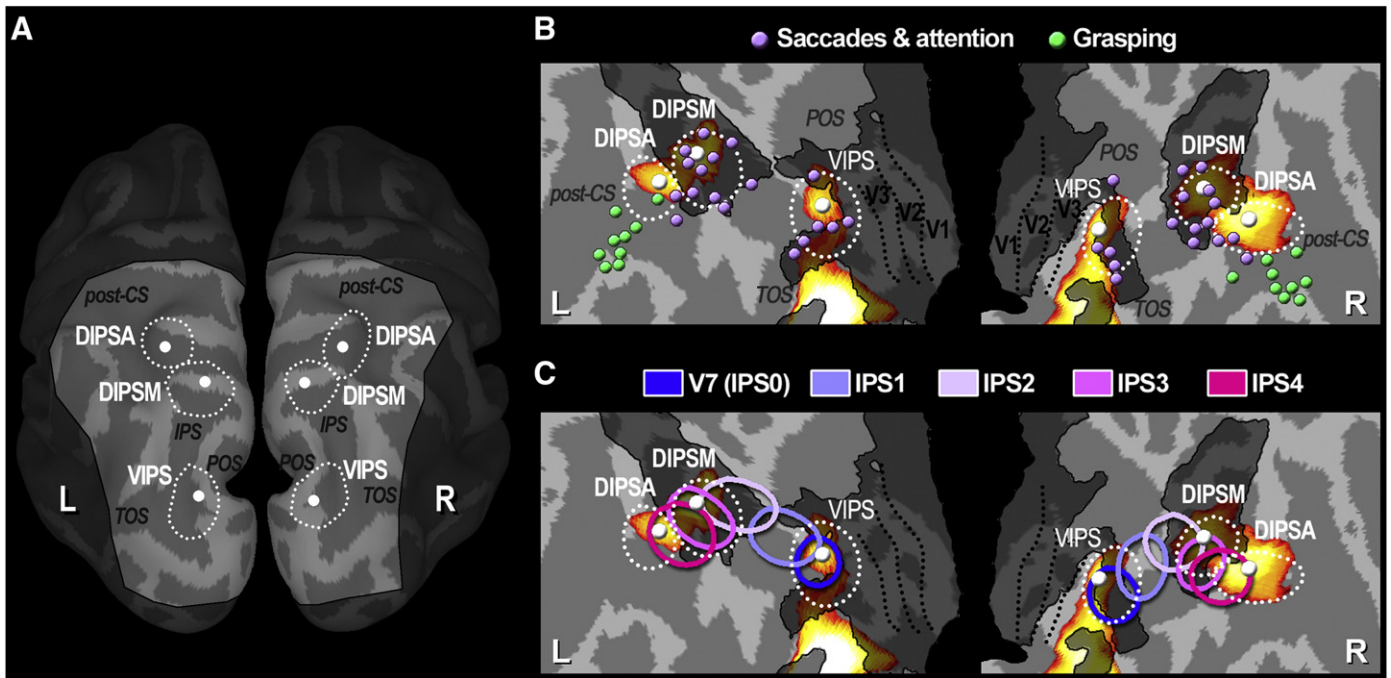
Fig. 8. (A) Postero-dorsal view of both left (L) and right (R) hemispheres showing the location of VIPS, DIPSM and DIPSA (white circular symbols) and their confidence intervals (white dotted ellipses) (B) Same as Fig. 7A with purple and green circular symbols indicating local maxima from previous studies respectively for tasks involving ocular saccades and/or spatial attention (Astafiev et al., 2003; Connolly et al., 2002; Corbetta et al., 1998; Koyama et al., 2004; Medendorp et al., 2005; Schluppeck et al., 2005; Sereno et al., 2001; Simon et al., 2002; Wojciulik and Kanwisher, 1999) and for motor tasks related to the grasping of objects (Begliomini et al., 2007; Binkofski et al., 1999; Binkofski et al., 1998; Cavina-Pratesi et al., 2007; Culham et al., 2003; Frey et al., 2005; Kroliczak et al., 2007). C. Same as Fig. 7A with ellipses indicating the location of V7, IPS1, IPS2, IPS3 and IPS4. Ellipses were drawn from the mean MNI coordinates (and standard deviations) reported by Swisher et al. (2007).

the Georgieva et al. (2009) study, hAIP did exhibit some 3D shape sensitivity but it was weaker than that in DIPSA. These findings lend support to the view (Culham et al., 2003; Orban et al., 2006) that DIPSA and hAIP may form the posterior (sensory-dominant) and anterior (motor-dominant) parts of human AIP respectively.

Several retinotopic areas have been reported in the human parietal cortex, even if their number and location are still controversial (Georgieva et al., 2009; Hagler et al., 2007; Jack et al., 2007; Konen and Kastner, 2008a; Sereno et al., 2001; Schluppeck et al., 2005; Silver et al., 2005; Swisher et al., 2007; Wandell et al., 2007). Most studies so far, with the exception of Georgieva et al. (2009), have mapped only the polar angle or used only polar maps to define cortical areas. Two cortical areas, that share meridians but have opposite eccentricity gradients, such as V3C and V3D in Georgieva et al. (2009), cannot be distinguished if only polar angle is mapped or used to define areas. Thus further effort is needed to determine the exact retinotopic organization of human parietal cortex. Fig. 8C indicates the four parietal regions IPS1–4, taken from the recent study of Swisher et al. (2007). These four regions are commonly reported when polar angle is mapped (Wandell et al., 2007). Comparing the confidence ellipses of DIPSM and DIPSA with those of IPS1–4 suggests that DIPSM and DIPSA may correspond to distinct retinotopic areas: IPS3 and IPS4 respectively (Fig. 8C). Swisher et al. (2007) have provided some indications that these two areas may share a representation of central vision.

Posterior parietal region

We found that visual 3D shape processing from disparity in contours also recruits a posterior parietal region (VIPS), in agreement with a previous study (Georgieva et al., 2009). The present study differentiates VIPS from DIPSA/DIPSM by a mixed sensitivity to visual shape and to position in depth (Table 1 and Fig. 2). Furthermore VIPS is separated from the anterior areas by a

region that is sensitive predominantly to position in depth. Thus random-line stimuli produce more differences in functional profiles related to 3D shape from disparity along the human IPS than textured surfaces do. In the motion domain, 3D structure from motion also activated human parietal regions differently depending on whether the stimuli were textured surfaces or random-line stimuli (Orban et al., 2006). One earlier fMRI study related to 3D shape processing reported similar functional properties along the whole extent of the IPS (Chandrasekaran et al., 2007), while other studies emphasized its functional heterogeneity (Konen and Kastner, 2008b; Shikata et al., 2008).

Fig. 8C clearly suggests that VIPS might correspond to V7 (Tootell et al., 1998) or equivalently IPS0 (Wandell et al., 2007). This is directly supported by the retinotopic mapping in Georgieva et al. (2009), who concluded that VIPS either corresponds to V7 itself or an area located deeper in the sulcus and sharing a central representation and meridians with V7 but having opposite eccentricity gradients. Hence they refer to this area as VIPS/V7*.

Homology with monkey parietal regions

Homology is difficult to establish when only functional data are available in two species. Even when restricting homology to a functional similarity, care has to be taken when using the same task in humans and monkeys. The two species may use different strategies to solve a similar task. Yet, in the present study, the tasks were extremely simple and at least the high-acuity and passive fixation tasks did not involve the 2D or 3D stimuli of interest. Therefore, the present results support the homology between anterior IPS regions in humans and macaque monkeys first proposed by Orban et al. (2006), i.e. that DIPSM and DIPSA correspond to macaque anterior LIP and posterior AIP respectively. DIPSM and DIPSA are sensitive to depth structure defined from disparity, both in connected random lines (present study) and in textured surfaces (Georgieva et al., 2009) as are

anterior LIP and posterior AIP (Durand et al., 2007). Both human regions are sensitive to 2D shape (Denys et al., 2004; Georgieva et al., 2009 and present study) as are the corresponding monkey regions (Denys et al., 2004; Durand et al., 2007) and this result does not depend on familiarity with the objects (Denys et al., 2004). Both human regions have a central representation (Orban et al., 2006), which they possibly share (Swisher et al., 2007), as do LIP and AIP (Ben Hamed et al., 2001; Fize et al., 2003). DIPSM but not DIPSA is sensitive to saccades (present study), as is the case for anterior LIP and not AIP (Durand et al., 2007). In addition these pairs of areas are located at the boundary between cortical regions activated by saccades and grasping movements, both in humans (Fig. 8A, Astafiev et al., 2003; Begliomini et al., 2007; Binkofski et al., 1999, 1998; Cavina-Pratesi et al., 2007; Connolly et al., 2002; Corbetta et al., 1998; Culham et al., 2003; Frey et al., 2005; Koyama et al., 2004; Kroliczak et al., 2007; Medendorp et al., 2005; Schluppeck et al., 2005; Sereno et al., 2001; Simon et al., 2002; Wojciulik and Kanwisher, 1999) and in macaques (Andersen et al., 1990; Gnadt and Andersen, 1988; Gottlieb et al., 1998; Murata et al., 2000; Snyder et al., 1997). Minor discrepancies involve the motion domain. DIPSM and DIPSA are sensitive to motion (Sunaert et al., 1999) and to 3D structure from motion (Orban et al., 1999; Vanduffel et al., 2002). Yet anterior LIP is sensitive to motion but AIP is not (Fanini and Assad, 2009; Orban et al., 2006). Conversely, AIP is weakly sensitive to 3D structure from motion, but LIP is not (Durand et al., 2007; Vanduffel et al., 2002). Just as there is some evidence that human AIP might have an anterior posterior gradient whereby the posterior part is more visual and the anterior part is more motor, monkey AIP might exhibit a similar gradient. The 3D random-line stimuli elicited activations that decreased in amplitude from the posterior to the anterior end of macaque AIP (see Figs. 2 and 7 in Durand et al., 2007). Furthermore the anatomical connections of the anterior part of AIP differ from those of the more posterior part (Lewis and Van Essen, 2000a).

The present results also suggest a possible homology between VIPS/V7* in humans and CIP in macaques, because both have a mixed sensitivity to depth structure and position in depth, and are located caudally in the IPS (Durand et al., 2007 and present study). This proposal only partially fits with that of Shikata et al. (2003, 2008), who located the human homologue of CIP more dorsally, close to POIPS (Orban et al., 1999; Sunaert et al., 1999). On the other hand, the random stereo checkerboards used by Tsao et al. (2003) activated CIP in the monkey and both V7 and more dorsal parietal regions in the humans. A further complication is that in the monkey CIP is located anterior to V3A (Sakata et al., 1998; Taira et al., 2000), while in the human the V3A complex is considerably enlarged and V7 is abuts V3C/D (Georgieva et al., 2009). The fact that VIPS is motion sensitive (Sunaert et al., 1999), while CIP is not (Orban et al., 2006), is only a weak argument against the proposed homology, since the same holds true for V3A in humans and monkeys (Tootell et al., 1997; Vanduffel et al., 2001). And it has been suggested that such functional modification of V3A might cause similar changes in the areas receiving input from V3A, such as CIP (Nakamura et al., 2001). On the other hand, CIP is located posterior to LIP (Sakata et al., 1998; Taira et al., 2000), and VIPS/V7* is located posterior to IPS1 and IPS2, which have frequently been proposed as the homologue of LIP, an area defined by saccadic and attention related tasks (Hagler et al., 2007; Saygin and Sereno, 2008; Schluppeck et al., 2006, 2005; Sereno et al., 2001; Silver et al., 2005). In a similar vein the region in monkey IPS between CIP and anterior LIP is sensitive mainly to position in depth from disparity (Durand et al., 2007) just as is the region in humans between VIPS and DIPSM (present study). Thus the homology between VIPS/V7* and CIP is plausible but needs to be confirmed by further experiments.

To conclude, we found that in humans, the extraction of 3D shape from disparity recruits anterior parietal regions DIPSM and DIPSA, whose functional properties and topographical arrangement are reminiscent of those encountered in the anterior LIP/posterior AIP complex of macaques, as well as a more posterior region, VIPS/V7*, the homology of which is less clear.

Acknowledgments

References

Andersen, R.A., Asanuma, C., Essick, G., Siegel, R.M., 1990. Corticocortical connections of anatomically and physiologically defined subdivisions within the inferior parietal lobule. J. Comp. Neurol. 296, 65–113.
Astafiev, S.V., Shulman, G.L., Stanley, C.M., Snyder, A.Z., Van Essen, D.C., Corbetta, M., 2003. Functional organization of human intraparietal and frontal cortex for attending, looking, and pointing. J. Neurosci. 23, 4689–4699.
Backus, B.T., Fleet, D.J., Parker, A.J., Heeger, D.J., 2001. Human cortical activity correlates with stereoscopic depth perception. J. Neurophysiol. 86, 2054–2068.
Baker, J.T., Patel, G.H., Corbetta, M., Snyder, L.H., 2006. Distribution of activity across the monkey cerebral cortical surface, thalamus and midbrain during rapid, visually guided saccades. Cereb. Cortex 16, 447–459.
Becker, W., 1989. Metrics. In: Wurtz, R.H., Goldberg, M.E. (Eds.), The Neurobiology of Saccade Eye Movements. Elsevier, Amsterdam, pp. 13–67.
Begliomini, C., Wall, M.B., Smith, A.T., Castiello, U., 2007. Differential cortical activity for precision and whole-hand visually guided grasping in humans. Eur. J. Neurosci. 25, 1245–1252.
Ben Hamed, S., Duhamel, J.R., Bremmer, F., Graf, W., 2001. Representation of the visual field in the lateral intraparietal area of macaque monkeys: a quantitative receptive field analysis. Exp. Brain Res. 140, 127–144.
Binkofski, F., Dohle, C., Posse, S., Stephan, K.M., Hefter, H., Seitz, R.J., Freund, H.J., 1998. Human anterior intraparietal area subserves prehension: a combined lesion and functional MRI activation study. Neurology 50, 1253–1259.
Binkofski, F., Buccino, G., Posse, S., Seitz, R.J., Rizzolatti, G., Freund, H., 1999. A fronto-parietal circuit for object manipulation in man: evidence from an fMRI-study. Eur. J. Neurosci. 11, 3276–3286.
Boltz, R.L., Harwerth, R.S., 1979. Fusional vergence ranges of the monkey: a behavioral study. Exp. Brain Res. 37, 87–91.
Borra, E., Belmalih, A., Calzavara, R., Gerbella, M., Murata, A., Rozzi, S., Luppino, G., 2008. Cortical connections of the macaque anterior intraparietal (AIP) area. Cereb. Cortex 18, 1094–1111.
Bremmer, F., Schlack, A., Shah, N.J., Zafiris, O., Kubischik, M., Hoffmann, K., Zilles, K., Fink, G.R., 2001. Polymodal motion processing in posterior parietal and premotor cortex: a human fMRI study strongly implies equivalencies between humans and monkeys. Neuron 29, 287–296.
Brouwer, G.J., van Ee, R., Schwarzbach, J., 2005. Activation in visual cortex correlates with the awareness of stereoscopic depth. J. Neurosci. 25, 10403–10413.
Cavina-Pratesi, C., Goodale, M.A., Culham, J.C., 2007. FMRI reveals a dissociation between grasping and perceiving the size of real 3D objects. PLoS ONE 2, e424.
Chandrasekaran, C., Canon, V., Dahmen, J.C., Kourtzi, Z., Welchman, A.E., 2007. Neural correlates of disparity-defined shape discrimination in the human brain. J. Neurophysiol. 97, 1553–1565.
Claeys, K.G., Lindsey, D.T., De Schutter, E., Orban, G.A., 2003. A higher order motion region in human inferior parietal lobule: evidence from fMRI. Neuron 40, 631–642.
Connolly, J.D., Goodale, M.A., Menon, R.S., Munoz, D.P., 2002. Human fMRI evidence for the neural correlates of preparatory set. Nat. Neurosci. 5, 1345–1352.
Corbetta, M., Shulman, G.L., 2002. Control of goal-directed and stimulus-driven attention in the brain. Nat. Rev., Neurosci. 3, 201–215.
Corbetta, M., Akbudak, E., Conturo, T.E., Snyder, A.Z., Ollinger, J.M., Drury, H.A., Linenweber, M.R., Petersen, S.E., Raichle, M.E., Van Essen, D.C., Shulman, G.L., 1998. A common network of functional areas for attention and eye movements. Neuron 21, 761–773.
Culham, J.C., Valyear, K.F., 2006. Human parietal cortex in action. Curr. Opin. Neurobiol. 16, 205–212.
Culham, J.C., Danckert, S.L., DeSouza, J.F., Gati, J.S., Menon, R.S., Goodale, M.A., 2003. Visually guided grasping produces fMRI activation in dorsal but not ventral stream brain areas. Exp. Brain Res. 153, 180–189.
Denys, K., Vanduffel, W., Fize, D., Nelissen, K., Peuskens, H., Van Essen, D., Orban, G.A., 2004. The processing of visual shape in the cerebral cortex of human and nonhuman primates: a functional magnetic resonance imaging study. J. Neurosci. 24, 2551–2565.
Durand, J.B., Nelissen, K., Vanduffel, W., Todd, J.T., Norman, J.F., Orban, G.A., 2006. Primate ips areas involved in visual 3D shape processing [Abstract]. Journal of Vision, 6(6):254, 254a, http://journalofvision.org/6/6/254/, doi:10.1167/6.6.254.
Durand, J.B., Nelissen, K., Joly, O., Wardak, C., Todd, J.T., Norman, J.F., Janssen, P., Vanduffel, W., Orban, G.A., 2007. Anterior regions of monkey parietal cortex process visual 3D shape. Neuron 55, 493–505.
Fanini, A., Assad, J.A., 2009. Direction selectivity of neurons in the macaque lateral intraparietal area. J. Neurophysiol. 101, 289–305.
Fize, D., Vanduffel, W., Nelissen, K., Denys, K., Chef d'Hotel, C., Faugeras, O., Orban, G.A., 2003. The retinotopic organization of primate dorsal V4 and surrounding areas: a

functional magnetic resonance imaging study in awake monkeys. J. Neurosci. 23, 7395–7406.

Frey, S.H., Vinton, D., Norlund, R., Grafton, S.T., 2005. Cortical topography of human anterior intraparietal cortex active during visually guided grasping. Brain Res. Cogn. Brain Res. 23, 397–405.

Friston, K.J., Holmes, A.P., Price, C.J., Buchel, C., Worsley, K.J., 1999. Multisubject fMRI studies and conjunction analyses. NeuroImage 10, 385–396.

Gauthier, I., Hayward, W.G., Tarr, M.J., Anderson, A.W., Skudlarski, P., Gore, J.C., 2002. BOLD activity during mental rotation and viewpoint-dependent object recognition. Neuron 34, 161–171.

Genovese, C.R., Lazar, N.A., Nichols, T., 2002. Thresholding of statistical maps in functional neuroimaging using the false discovery rate. NeuroImage 15, 870–878.

Georgieva, S.S., Todd, J.T., Peeters, R., Orban, G.A., 2008. The extraction of 3D shape from texture and shading in the human brain. Cereb. Cortex 18, 2416–2438.

Georgieva, S., Peeters, R., Kriegeskorte, N., Todd, J.T., Orban, G.A., 2009. The processing of three-dimensional shape from disparity in the human brain. J. Neurosci. 29, 727–742.

Gilaie-Dotan, S., Ullman, S., Kushnir, T., Malach, R., 2002. Shape-selective stereo processing in human object-related visual areas. Hum. Brain Mapp. 15, 67–79.

Gnadt, J.W., Mays, L.E.L., 1995. Neurons in monkey parietal area LIP are tuned for eye-movement parameters in three-dimensional space. J. Neurophysiol. 73, 280–297.

Gnadt, J.W., Andersen, R.A., 1988. Memory related motor planning activity in posterior parietal cortex of macaque. Exp. Brain Res. 70, 216–220.

Gottlieb, J.P., Kusunoki, M., Goldberg, M.E., 1998. The representation of visual salience in monkey parietal cortex. Nature 391, 481–484.

Grefkes, C., Fink, G.R., 2005. The functional organization of the intraparietal sulcus in humans and monkeys. J. Anat. 207, 3–17.

Grefkes, C., Weiss, P.H., Zilles, K., Fink, G.R., 2002. Crossmodal processing of object features in human anterior intraparietal cortex: an fMRI study implies equivalencies between humans and monkeys. Neuron 35, 173–184.

Hagler Jr., D.J., Riecke, L., Sereno, M.I., 2007. Parietal and superior frontal visuospatial maps activated by pointing and saccades. NeuroImage 35, 1562–1577.

Jack, A.I., Patel, G.H., Astafiev, S.V., Snyder, A.Z., Akbudak, E., Shulman, G.L., Corbetta, M., 2007. Changing human visual field organization from early visual to extra-occipital cortex. PLoS ONE 2, e452.

Janssen, P., Srivastava, S., Ombelet, S., Orban, G.A., 2008. Coding of shape and position in macaque lateral intraparietal area. J. Neurosci. 28, 6679–6690.

Joly, O., Vanduffel, W., Orban, G.A., 2007. Visual 3D Shape Processing from Disparity in the Frontal Lobe: fMRI Evidence from Awake Monkeys. Program No. 716.10. Neuroscience Meeting Planner. Society for Neuroscience, San Diego, CA. 2007. Online.

Kanwisher, N., Wojciulik, E., 2000. Visual attention: insights from brain imaging. Nat. Rev., Neurosci. 1, 91–100.

Konen, C.S., Kastner, S., 2008a. Representation of eye movements and stimulus motion in topographically organized areas of human posterior parietal cortex. J. Neurosci. 28, 8361–8375.

Konen, C.S., Kastner, S., 2008b. Two hierarchically organized neural systems for object information in human visual cortex. Nat. Neurosci. 11, 224–231.

Kourtzi, Z., Kanwisher, N., 2000. Cortical regions involved in perceiving object shape. J. Neurosci. 20, 3310–3318.

Kourtzi, Z., Erb, M., Grodd, W., Bulthoff, H.H., 2003. Representation of the perceived 3-D object shape in the human lateral occipital complex. Cereb. Cortex 13, 911–920.

Koyama, M., Hasegawa, I., Osada, T., Adachi, Y., Nakahara, K., Miyashita, Y., 2004. Functional magnetic resonance imaging of macaque monkeys performing visually guided saccade tasks: comparison of cortical eye fields with humans. Neuron 41, 795–807.

Kroliczak, G., Cavina-Pratesi, C., Goodman, D.A., Culham, J.C., 2007. What does the brain do when you fake it? An FMRI study of pantomimed and real grasping. J. Neurophysiol. 97, 2410–2422.

Lehky, S.R., Sereno, A.B., 2007. Comparison of shape encoding in primate dorsal and ventral visual pathways. J. Neurophysiol. 97, 307–319.

Lewis, J.W., Van Essen, D.C., 2000a. Corticocortical connections of visual, sensorimotor, and multimodal processing areas in the parietal lobe of the macaque monkey. J. Comp. Neurol. 428, 112–137.

Lewis, J.W., Van Essen, D.C., 2000b. Mapping of architectonic subdivisions in the macaque monkey, with emphasis on parieto-occipital cortex. J. Comp. Neurol. 428, 79–111.

Li, G., Zucker, S.W., 2006a. Contextual inference in contour-based stereo correspondence. Int. J. Comput. Vis. 69, 59–75.

Li, G., Zucker, S.W., 2006b. Differential geometric consistency extends stereo to curved surfaces. In: Springer (Ed.), Proc. European Conference on Computer Vision (ECCV'06). Graz, Austria, pp. 44–57.

Luppino, G., Murata, A., Govoni, P., Matelli, M., 1999. Largely segregated parietofrontal connections linking rostral intraparietal cortex (areas AIP and VIP) and the ventral premotor cortex (areas F5 and F4). Exp. Brain Res. 128, 181–187.

Medendorp, W.P., Goltz, H.C., Crawford, J.D., Vilis, T., 2005. Integration of target and effector information in human posterior parietal cortex for the planning of action. J. Neurophysiol. 93, 954–962.

Murata, A., Gallese, V., Luppino, G., Kaseda, M., Sakata, H., 2000. Selectivity for the shape, size, and orientation of objects for grasping in neurons of monkey parietal area AIP. J. Neurophysiol. 83, 2580–2601.

Murray, S.O., Olshausen, B.A., Woods, D.L., 2003. Processing shape, motion and three-dimensional shape-from-motion in the human cortex. Cereb. Cortex 13, 508–516.

Nakamura, H., Kuroda, T., Wakita, M., Kusunoki, M., Kato, A., Mikami, A., Sakata, H., Itoh, K., 2001. From three-dimensional space vision to prehensile hand movements: the lateral intraparietal area links the area V3A and the anterior intraparietal area in macaques. J. Neurosci. 21, 8174–8187.

Neri, P., Bridge, H., Heeger, D.J., 2004. Stereoscopic processing of absolute and relative disparity in human visual cortex. J. Neurophysiol. 92, 1880–1891.

Orban, G.A., Sunaert, S., Todd, J.T., Van Hecke, P., Marchal, G., 1999. Human cortical regions involved in extracting depth from motion. Neuron 24, 929–940.

Orban, G.A., Fize, D., Peuskens, H., Denys, K., Nelissen, K., Sunaert, S., Todd, J., Vanduffel, W., 2003. Similarities and differences in motion processing between the human and macaque brain: evidence from fMRI. Neuropsychologia 41, 1757–1768.

Orban, G.A., Claeys, K., Nelissen, K., Smans, R., Sunaert, S., Todd, J.T., Wardak, C., Durand, J.B., Vanduffel, W., 2006. Mapping the parietal cortex of human and non-human primates. Neuropsychologia 44, 2647–2667.

Pitzalis, S., Galletti, C., Huang, R.S., Patria, F., Committeri, G., Galati, G., Fattori, P., Sereno, M.I., 2006. Wide-field retinotopy defines human cortical visual area v6. J. Neurosci. 26, 7962–7973.

Preston, T.J., Li, S., Kourtzi, Z., Welchman, A.E., 2008. Multivoxel pattern selectivity for perceptually relevant binocular disparities in the human brain. J. Neurosci. 28, 11315–11327.

Price, C.J., Friston, K.J., 1997. Cognitive conjunction: a new approach to brain activation experiments. NeuroImage 5, 261–270.

Rombouts, S.A., Barkhof, F., Hoogenraad, F.G., Sprenger, M., Scheltens, P., 1998. Within-subject reproducibility of visual activation patterns with functional magnetic resonance imaging using multislice echo planar imaging. Magn. Reson. Imaging 16, 105–113.

Sakata, H., Taira, M., Murata, A., Mine, S., 1995. Neural mechanisms of visual guidance of hand action in the parietal cortex of the monkey. Cereb. Cortex 5, 429–438.

Sakata, H., Taira, M., Kusunoki, M., Murata, A., Tanaka, Y., Tsutsui, K., 1998. Neural coding of 3D features of objects for hand action in the parietal cortex of the monkey. Philos. Trans. R. Soc. Lond., B. Biol. Sci. 353, 1363–1373.

Sawamura, H., Georgieva, S., Vogels, R., Vanduffel, W., Orban, G.A., 2005. Using functional magnetic resonance imaging to assess adaptation and size invariance of shape processing by humans and monkeys. J. Neurosci. 25, 4294–4306.

Saygin, A.P., Sereno, M.I., 2008. Retinotopy and attention in human occipital, temporal, parietal, and frontal cortex. Cereb. Cortex 18, 2158–2168.

Schluppeck, D., Glimcher, P., Heeger, D.J., 2005. Topographic organization for delayed saccades in human posterior parietal cortex. J. Neurophysiol. 94, 1372–1384.

Schluppeck, D., Curtis, C.E., Glimcher, P.W., Heeger, D.J., 2006. Sustained activity in topographic areas of human posterior parietal cortex during memory-guided saccades. J. Neurosci. 26, 5098–5108.

Sereno, A.B., Maunsell, J.H., 1998. Shape selectivity in primate lateral intraparietal cortex. Nature 395, 500–503.

Sereno, M.I., Pitzalis, S., Martinez, A., 2001. Mapping of contralateral space in retinotopic coordinates by a parietal cortical area in humans. Science 294, 1350–1354.

Shikata, E., Hamzei, F., Glauche, V., Koch, M., Weiller, C., Binkofski, F., Buchel, C., 2003. Functional properties and interaction of the anterior and posterior intraparietal areas in humans. Eur. J. Neurosci. 17, 1105–1110.

Shikata, E., McNamara, A., Sprenger, A., Hamzei, F., Glauche, V., Buchel, C., Binkofski, F., 2008. Localization of human intraparietal areas AIP, CIP, and LIP using surface orientation and saccadic eye movement tasks. Hum. Brain Mapp. 29, 411–421.

Silver, M.A., Ress, D., Heeger, D.J., 2005. Topographic maps of visual spatial attention in human parietal cortex. J. Neurophysiol. 94, 1358–1371.

Simon, O., Mangin, J.F., Cohen, L., Le Bihan, D., Dehaene, S., 2002. Topographical layout of hand, eye, calculation, and language-related areas in the human parietal lobe. Neuron 33, 475–487.

Snyder, L.H., Batista, A.P., Andersen, R.A., 1997. Coding of intention in the posterior parietal cortex. Nature 386, 167–170.

Srivastava, S., Orban, G.A., Janssen, P., 2006. Selectivity for Three-Dimensional Shape in Macaque Posterior Parietal Cortex. Program No. 407.9. Neuroscience Meeting Planner. Society for Neuroscience, Atlanta, GA. 2006. Online.

Srivastava, S., Orban, G.A., Janssen, P., 2007. Coding for First- and Second Order Disparity in Macaque Posterior Parietal Cortex. Program No. 716.7. Neuroscience Meeting Planner. Society for Neuroscience, San Diego, CA. 2007. Online.

Sunaert, S., Van Hecke, P., Marchal, G., Orban, G.A., 1999. Motion-responsive regions of the human brain. Exp. Brain Res. 127, 355–370.

Swisher, J.D., Halko, M.A., Merabet, L.B., McMains, S.A., Somers, D.C., 2007. Visual topography of human intraparietal sulcus. J. Neurosci. 27, 5326–5337.

Taira, M., Mine, S., Georgopoulos, A.P., Murata, A., Sakata, H., 1990. Parietal cortex neurons of the monkey related to the visual guidance of hand movement. Exp. Brain Res. 83, 29–36.

Taira, M., Tsutsui, K.I., Jiang, M., Yara, K., Sakata, H., 2000. Parietal neurons represent surface orientation from the gradient of binocular disparity. J. Neurophysiol. 83, 3140–3146.

Tootell, R.B., Mendola, J.D., Hadjikhani, N.K., Ledden, P.J., Liu, A.K., Reppas, J.B., Sereno, M.I., Dale, A.M., 1997. Functional analysis of V3A and related areas in human visual cortex. J. Neurosci. 17, 7060–7078.

Tootell, R.B., Hadjikhani, N., Hall, E.K., Marrett, S., Vanduffel, W., Vaughan, J.T., Dale, A.M., 1998. The retinotopy of visual spatial attention. Neuron 21, 1409–1422.

Tsao, D.Y., Vanduffel, W., Sasaki, Y., Fize, D., Knutsen, T.A., Mandeville, J.B., Wald, L.L., Dale, A.M., Rosen, B.R., Van Essen, D.C., Livingstone, M.S., Orban, G.A., Tootell, R.B., 2003. Stereopsis activates V3A and caudal intraparietal areas in macaques and humans. Neuron 39, 555–568.

Tsutsui, K., Sakata, H., Naganuma, T., Taira, M., 2002. Neural correlates for perception of 3D surface orientation from texture gradient. Science 298, 409–412.

Tyler, C.W., Likova, L.T., Kontsevich, L.L., Wade, A.R., 2006. The specificity of cortical region KO to depth structure. NeuroImage 30, 228–238.

Van Essen, D.C., 2004. Organization of visual areas in macaque and human cerebral cortex. In: Chalupa, L., Werner, J.S. (Eds.), The Visual Neurosciences. MIT Press, pp. 507–521.

Van Essen, D.C., 2005. A Population-Average, Landmark- and Surface-based (PALS) atlas of human cerebral cortex. NeuroImage 28, 635–662.

Van Essen, D.C., Drury, H.A., Dickson, J., Harwell, J., Hanlon, D., Anderson, C.H., 2001. An integrated software suite for surface-based analyses of cerebral cortex. J. Am. Med. Inform. Assoc. 8, 443–459.

Vanduffel, W., Fize, D., Mandeville, J.B., Nelissen, K., Van Hecke, P., Rosen, B.R., Tootell, R.B., Orban, G.A., 2001. Visual motion processing investigated using contrast agent-enhanced fMRI in awake behaving monkeys. Neuron 32, 565–577.

Vanduffel, W., Fize, D., Peuskens, H., Denys, K., Sunaert, S., Todd, J.T., Orban, G.A., 2002. Extracting 3D from motion: differences in human and monkey intraparietal cortex. Science 298, 413–415.

Wandell, B.A., Dumoulin, S.O., Brewer, A.A., 2007. Visual field maps in human cortex. Neuron 56, 366–383.

Welchman, A.E., Deubelius, A., Conrad, V., Bulthoff, H.H., Kourtzi, Z., 2005. 3D shape perception from combined depth cues in human visual cortex. Nat. Neurosci. 8, 820–827.

Wojciulik, E., Kanwisher, N., 1999. The generality of parietal involvement in visual attention. Neuron 23, 747–764.